

High-throughput sorting and analysis of human sperm with a ring-shaped laser trap

Bing Shao · Linda Z. Shi · Jaclyn M. Nascimento ·
Elliot L. Botvinick · Mihrimah Ozkan ·
Michael W. Berns · Sadik C. Esener

Published online: 17 January 2007
© Springer Science + Business Media, LLC 2007

Abstract Sperm motility is an important concept in fertility research. To this end, single spot laser tweezers have been used to quantitatively analyze the motility of individual sperm. However, this method is limited with throughput (single sperm per spot), lacks the ability of *in-situ* sorting based on motility and chemotaxis, requires high laser power (hundreds of milliWatts) and can not be used to dynamically monitor changes in sperm swimming behavior under the influence of a laser beam. Here, we report a continuous 3-D ring-shaped laser trap which could be used for multi-level and high-throughput (tens to hundred sperm per ring) sperm sorting based on their motility and chemotaxis. Under a laser power of only tens of milliWatts, human sperm with low to medium velocity are slowed down, stopped, or forced to change their trajectories to swim along the ring due to the optical gradient force in the radial direction. This is the first demonstration of parallel sperm sorting based on motility with optical trapping technology. In addition, by making the

sperm swimming along the circumference of the ring, the effect of laser radiation, optical force and external obstacles on sperm energetics are investigated in a more gentle and quantitative way. The application of this method could be extended to motility and bio-tropism studies of other self-propelled cells, such as algae and bacteria.

Keywords Laser trapping · Sperm motility · Cell sorting · Axicon

1 Introduction

Artificial insemination (AI) has been of great practical importance in animal husbandry and in the effort to preserve endangered species. The overall quality of the sperm to be used is among the most critical factors in an effective AI program, which makes sperm assessment an essential procedure before cryopreservation. Noninvasive and high throughput analysis of sperm motility is crucial for successful artificial insemination and genetic improvement programs. Conventional technologies use a microscope to evaluate one sperm at a time subjectively and qualitatively, which is labor intensive and lacks a universal standard. These considerations give rise to a strong need for an automated, quantitative, and objective assessment tool for sperm quality. In the last 25 years, computer aided sperm analysis (CASA) has been developed to offer objective assessment of sperm motility for large populations. However, the thin chambers (30 μm) used in CASA may affect the behavior of sperm that swim with large transverse amplitudes (e.g. monkey sperm) (Baumber and Meyers, 2006), and the errors encountered by CASA when dealing with phase contrast images often lead to errors in the actual sperm number detected in the field. Finally, while CASA can measure the motility

B. Shao (✉) · S. C. Esener
Department of Electrical and Computer Engineering,
University of California, San Diego,
La Jolla, CA 92093, USA
e-mail: bingshaoucsd@gmail.com

L. Z. Shi · J. M. Nascimento
Department of Bioengineering, University of California,
San Diego, La Jolla, CA 92093, USA

E. L. Botvinick · M. W. Berns
Department of Biomedical Engineering, Beckman Laser Institute,
University of California, Irvine,
Irvine, CA 92612, USA

M. Ozkan
Department of Electrical Engineering, University of California,
Riverside, Riverside, CA 92521, USA

of sperm, it can not provide information on swimming force that is potentially useful in the assessment of sperm viability.

Optical tweezers have been used to study laser-sperm interactions and sperm motility by measuring the swimming force generated by a sperm (Konig et al., 1996; Araujo et al., 1994; Dantas et al., 1995; Patrizio et al., 2000; Tadir et al., 1989, 1990). These studies determined that the minimal laser power needed to hold a sperm in the trap (threshold escape power) is directly proportional to the sperm's swimming force. They also revealed a relationship between sperm motility and swimming pattern (Tadir et al., 1990), and investigated the medical aspects of sperm activity (Dantas et al., 1995; Patrizio et al., 2000).

Single spot laser tweezers provides a quantitative analysis of individual sperm motility, nevertheless it has some drawbacks. Firstly, it still analyzes one sperm at a time. Therefore it is limited in throughput. Secondly, it lacks the ability of *in-situ* sorting based on motility. Thirdly, it has difficulty in assessing the role of chemotaxis—sperm-egg communication which may help to explain infertility and provide new approaches to contraception (Eisenbach and Tur-Kaspa, 1999). Finally, it measures sperm by stopping it completely, thus it can not be used to dynamically monitor the change in swimming behavior when a sperm is exposed to the trapping laser beam.

In this paper, we present a 3-D annular laser trap which could be used for parallel sperm sorting based on motility and chemotaxis. For the first time, two-level sperm sorting

based on motility is demonstrated with this novel technology. Different from the single spot laser trap which focuses hundreds of milliwatts to immobilize a sperm, the ring-shaped trap distributes only tens of milliwatts on a sperm, allowing the sperm to swim along the ring without having to come to a complete stop. As a result, the effect of optical force, laser radiation and even external obstacles on sperm swimming pattern can be investigated in more detail.

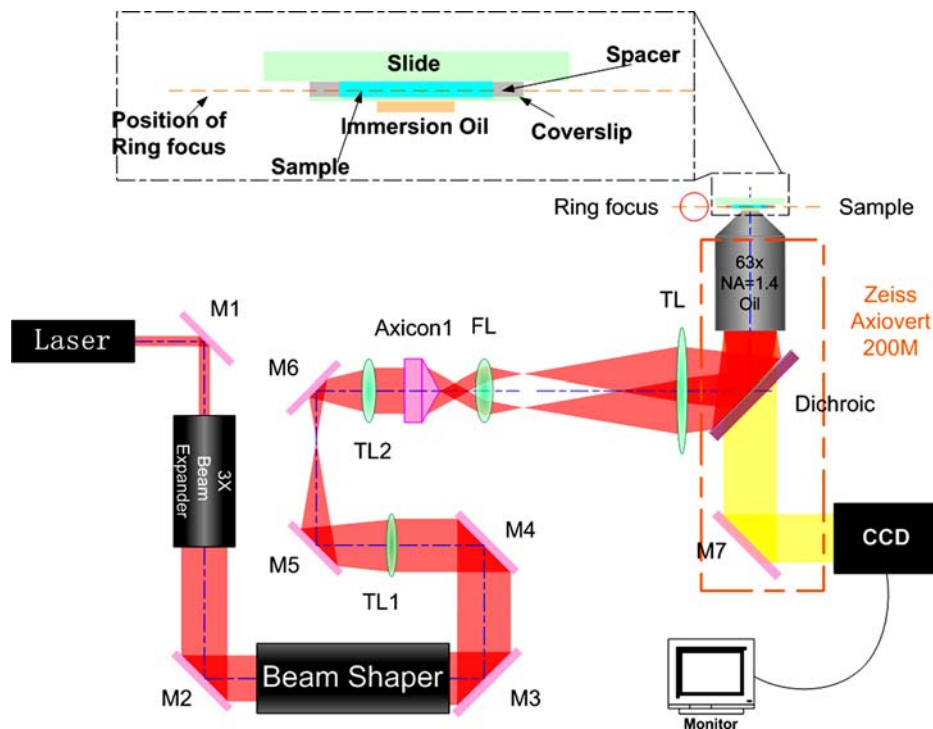
In contrast to other approaches for creating an annular trap, such as generalized phase contrast (GPC) that needs counter-propagating beams for 3-D confinement (Rodrigo et al., 2004), holographic optical trapping (HOT) that generally suffers from low diffraction efficiency and needs high resolution spatial light modulator (SLM) (Lafong et al., 2006), our system utilizes the special optical properties of an axicon—an optical element with a conical surface that generates a ring-shaped focus when working with a positive lens—to create a continuous annular trap with 3-D trapping ability and almost 100% power efficiency. In addition, it is free from mechanical scan, which introduces a tangential drag force on the sample (Wang et al., 2003).

2 Materials and methods

2.1 Experimental setup

The annular laser trapping system, as shown in Fig. 1, consisted of a CW Ytterbium fiber laser with 1070 nm

Fig. 1 The schematic diagram of the annular laser trapping system. M1–M7—Mirrors, TL1—Telescope lens 1, TL2—Telescope lens 2, FL—focusing lens, TL—Tube lens



wavelength (PYL-20M, IPG Photonics, Oxford, MA). The laser beam is collimated and expanded via a $3 \times$ beam expander (T81-3X, Newport Corp., Irvine, CA). For better performance of the trap, a refractive beam shaper (GBS-AR14, Newport Corp., Irvine, CA) is used to convert a Gaussian laser beam into a collimated flat top beam (Shao, 2006). A telescope lens pair shrinks the beam to make the thickness of the light cone input to the objective equal to the diameter of the back aperture. In this way the numerical aperture of the trapping beam is maximized and the input laser power is fully utilized. An axicon-lens pair (axicon1-FL) is used to generate an annular focus that is conjugate to the ring-shaped trap at the specimen plane. After the tube lens (TL), the laser beam is sent into an inverted microscope (Axiovert 200M, Zeiss, Germany), and directed to the objective ($63 \times$ oil immersion, NA = 1.4, Zeiss, Germany) by a side-facing dichroic mirror. The ring-shaped trap obtained at the specimen plane has a diameter of $120 \mu\text{m}$, which could accommodate up to 70 human sperm, whose head diameter is approximately $5 \mu\text{m}$.

2.2 Specimen

Human sperm (IGO medical group, San Diego, CA) were collected from donors and cryopreserved (stored in liquid N_2 (77 K)) according to a published protocol (DiMarzo et al., 1990; The Ethics Committee of the American Fertility Society, 1990; Serfini and Marrs, 1986) until needed for experimentation. After being thawed in a pre-warmed water bath (37°C) for approximately 10 min, sperm were transferred to an Eppendorf centrifuge tube. The following twice wash protocol was used to isolate the sperm (DiMarzo and Rakoff, 1986; Toffle et al., 1985). The sample was centrifuged at 2000 rpm for 10 min (centrifuge tip radius was 8.23 cm). The supernatant was removed and the remaining sperm pellet was re-suspended in 1 milliliter of pre-warmed HTF (HEPES Buffered Human Tubal Fluid) with 5% SSS (Serum Substitute Supplement, Irvine Scientific, Santa Ana, CA). The process was repeated a second time.

The specimen was loaded into a $120\text{-}\mu\text{m}$ -thick chamber with a glass slide as the top and a No.1 cover-slip as the bottom. The sample was mounted into a microscope stage holder and kept at room temperature during the experiment.

3 Results

3.1 Sperm sorting based on motility

Firstly, we demonstrate sperm sorting with the annular trap according to their motility parameters. Curvilinear velocity (VCL), smooth path velocity (VAP) and amplitude of lateral head displacement (ALH) were measured using custom

software that tracks the sperm (Shi et al., 2005). With an estimated laser power of 25 mW per sperm (total power in the specimen plane divided by the maximal number of sperm the ring could accommodate), the tested sperm could be classified into two groups according to their responses to the ring-shaped trap. The first group, or the “fast” group, is defined as sperm that swim through the ring with no detectable speed reduction. The second group, or the “slow” group, represents sperm whose swimming pattern is considerably affected by the ring, i.e., those that are slowed down, those that experience a temporary or permanent loss of motility, or those that change their swimming trajectories. As seen in Fig. 2, the “fast” group has much higher average VCL and VAP than the “slow” one, while their ALH are very close. The unpaired student T-test shows a p -value of 1.2×10^{-15} for VCL, 1.2×10^{-16} for VAP, and 0.3 for ALH, which means the “fast” group could be significantly differentiated from the “slow” group with a very high ($> 99.99\%$) confidence according to VAP or VCL, whereas ALH is a much less reliable way of discriminating between the two groups. Figure 3 is a video frame showing multiple sperm stopped by the ring.

3.2 Sperm dynamic analysis

The effect of the annular laser trap on sperm motility was studied by making sperm swim along the curvature of the ring (Fig. 4). Because of the optical properties of an axicon, the gradient force of the annular laser trap is only in the radial direction. Trapped particles thus are free to move along the circumference as long as their tangential movement is not based on their radial action. However, for flagellated cells like sperm, forward movement results from the viscous interactions of flagellum with the medium (Taylor, 1951), which includes lateral beating. Therefore, the radial confinement to a sperm that swims along the ring should reduce its motility. To test this hypothesis, laser power is adjusted so that the swimming pattern of a sperm under different amounts of optical force and illumination is examined.

Five types of observations were made, which are identified as “power binary”, “power gradient”, “fatigue”, “load” and “block”. In “power binary”, the laser is switched on and off so that the swimming parameters are measured for a sperm while it is propelling along the ring and after it is released from the trap. “Power gradient” measures the change of sperm swimming pattern as a result of the decay of the laser power. “Fatigue” examines the slowing down of a sperm after it is guided along the ring under a fixed trapping power for an extended period of time. “Load” means a sperm is swimming along the ring while pushing an object, such as a dead sperm or cell debris. Finally, “block” studies the behavior of a sperm while its forward movement is interrupted by an external obstacle.

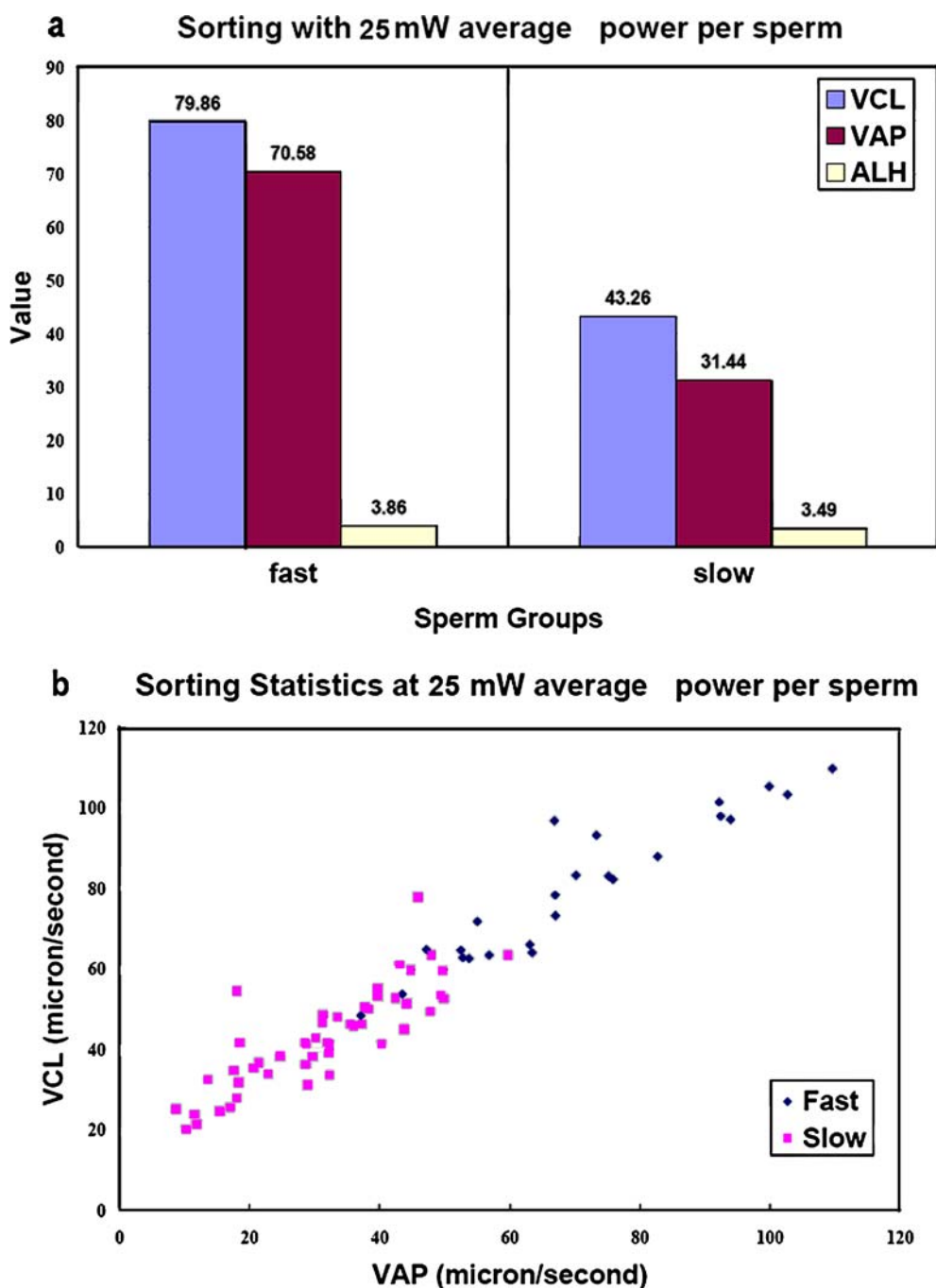


Fig. 2 Parallel sperm sorting with annular laser trap when the estimated average laser power is 25 mW per sperm. (a) The mean value of VCL, VAP and ALH for “fast” and “slow” sperm from a population of 83 sperm. (b) The statistics VCL and VAP distribution of all the 83 sperm

A total of 93 sperm were measured, and for each sperm one or more types of observations were made. For “power binary”, the percentages of sperm exhibiting a higher motility parameter while freely swimming are 79.33% for VAP, 75.69% for VCL, but only 42.66% for ALH. For “power gradient”, most sperm experience increased VAP (76.03%) or VCL (73.97%) with decreased trapping power, while only 44.61% show an ALH increase with power decay. Among all the observations of “fatigue”, with increased time (typically

after 15–20 s along the ring), 80.95% have a reduced VAP, 76.19% have a reduced ALH, and 100% have a reduced VCL. Observations of “load” yield reduction of VAP and VCL in 100% of the tested sperm, whereas ALH reduction is seen in only 75% of the sperm. 100% of the sperm “blocked” by a dead sperm or a red blood cell show a decrease in VAP, VAL and ALH.

Figure 5(a) shows a repeatable reduction and recovery of VAP, VCL, and ALH as the sperm was swimming along

Fig. 3 Tens of sperm are stopped along the ring focus

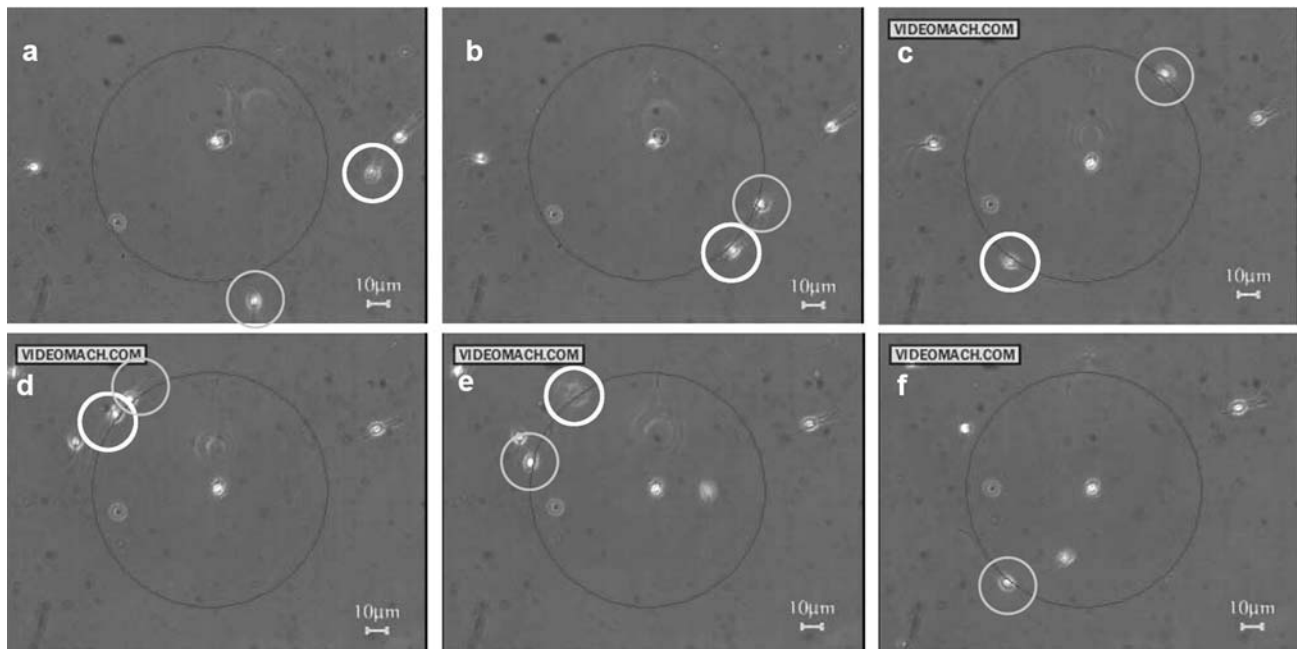
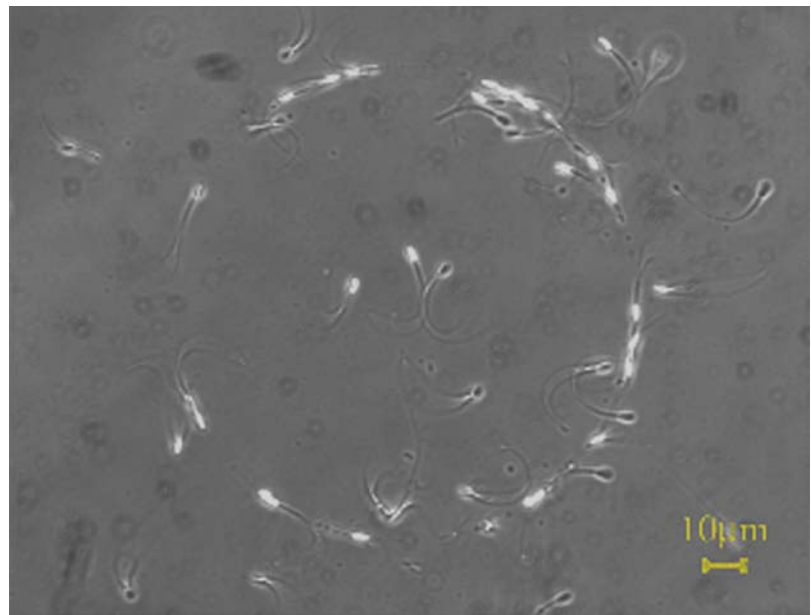


Fig. 4 Guiding two sperm along the ring under an estimated average laser power of 25 mW per sperm. (a) Two sperm are freely swimming in opposite directions close to the ring (big dark circle). (b) Affected by the optical gradient force from the ring trap, the two sperm start swimming along the curvature of the ring, one clockwise (small white circle), the

other counterclockwise (small grey circle). (c) The two sperm continue swimming in opposite direction. (d) After swimming along the ring for about 180°, the two sperm are about to collide with each other. (e, f), After collision, one sperm (small white circle) is knocked out of the focus, while the other (small grey circle) keep swimming along the ring

and released from the ring trap. The average trapping power per sperm was switched between 25 mW and 0 mW. The amounts of reduction and recovery were almost constant for VAP and VCL, while they were less predictable for ALH. In Fig. 5(b), VAP and VCL increased as a result of power decay, however, ALH failed to increase after the power was reduced to 11 mW. As an example of “fatigue”, the sperm in Fig. 5(c) experienced a decrease of VAP and VCL after swimming

along the ring under an average laser power of 25 mW for more than 20 sec. Nevertheless, when the laser was turned off, both VAP and VCL showed a significant amount of recovery. Interestingly, the measured ALH followed an almost opposite trend with respect to the VAP and VCL. Figures 5(d) and (e) illustrate the response of a sperm to an obstacle when its swimming path was confined by the ring trap. In each case, a sperm was swimming along the ring, and en-

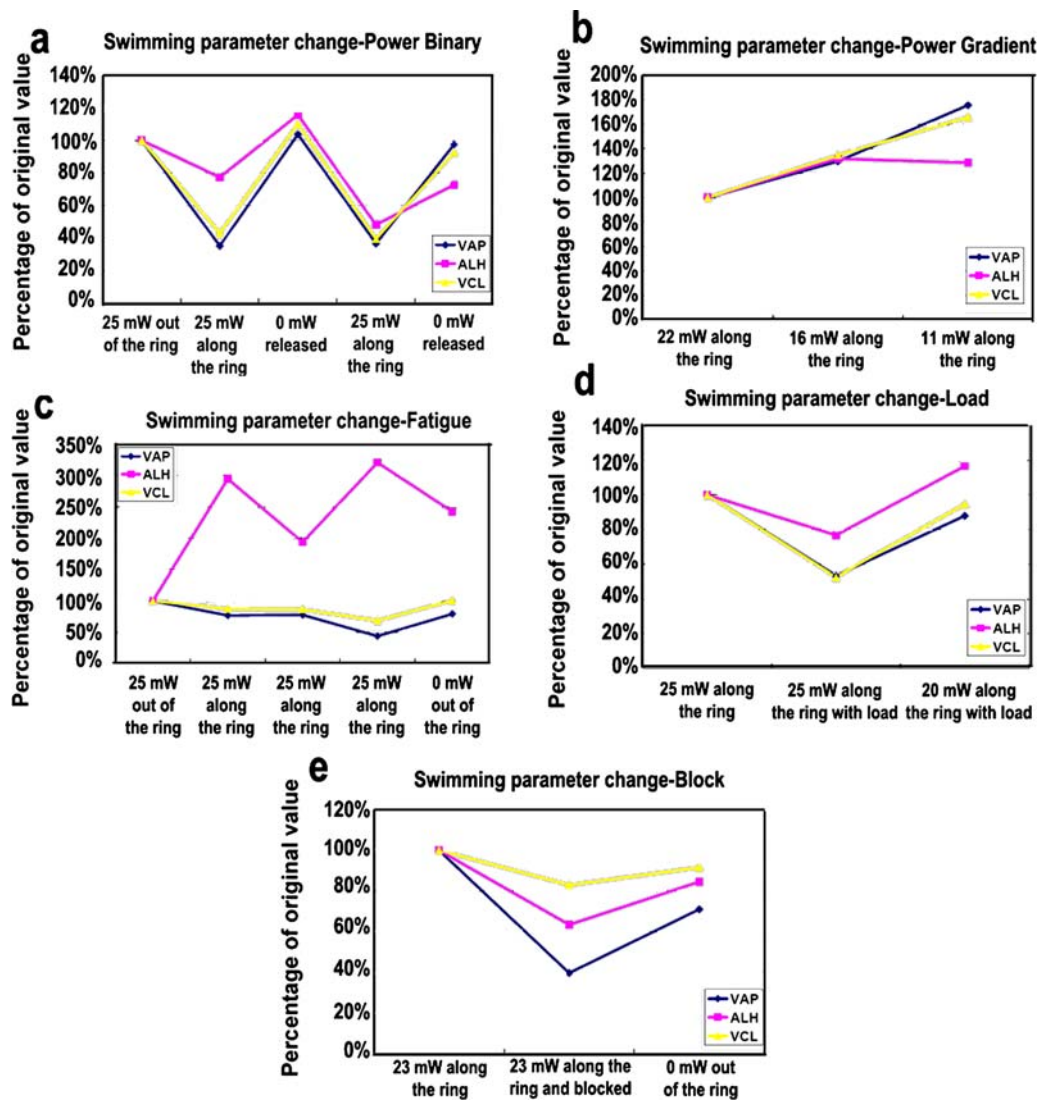


Fig. 5 Swimming parameter change in examples of the five types of observations. (a) “Power binary”, where a repeatable reduction/recovery of VAP, VCL, and ALH is observed as the sperm is swimming along/released from the ring trap. Original (100%) values: VAP—38 $\mu\text{m/s}$, ALH—4 μm , VCL—50 $\mu\text{m/s}$. (b) “Power gradient”, where an increase of VAP and VCL is observed with a decrease of the trapping power. Original (100%) values: VAP—17 $\mu\text{m/s}$, ALH—4 μm , VCL—28 $\mu\text{m/s}$. (c) “Fatigue”, where a decrease of VAP and VCL is observed after the sperm is swimming along the ring for more than 20 sec. Both VAP and VCL increase after the sperm is released. Original

(100%) values: VAP—40 $\mu\text{m/s}$, ALH—1 μm , VCL—41 $\mu\text{m/s}$. (d) “Load”, where a decrease of VAP, VCL and ALH is observed after the sperm starts pushing cell debris while swimming along the ring. All three parameters increase when the trapping power is decreased. Original (100%) values: VAP—14 $\mu\text{m/s}$, ALH—4 μm , VCL—36 $\mu\text{m/s}$. (e) “Block”, where a decrease of VAP, VCL and ALH is observed after the sperm’s forward movement along the ring is stopped by a dead sperm. All three parameters increase when the sperm is released. Original (100%) values: VAP—12 $\mu\text{m/s}$, ALH—4 μm , VCL—27 $\mu\text{m/s}$

countered an obstacle (cell debris or dead sperm) trapped by the ring. Due to the radial confinement introduced by the ring trap, the sperm did not have enough energy to escape the ring and detour around the obstacle. As a result, it tried to proceed by pushing the obstacle. For the case shown in Fig. 5(d), the obstacle was light so that the sperm was able to push it and continue swimming along the ring with a lower VAP, VCL and ALH. When the trapping power was reduced from 25 mW to 20 mW per sperm, all three parameters increased. In Fig. 5(e), the obstacle was heavy enough to stop

the sperm from proceeding. The sperm was struggling with reduced VAP, VCL and ALH. As soon as the laser was turned off, the sperm picked up its velocity and lateral head displacement, bypassed the obstacle, and swam away. In Figs. 6 and 7, the video frames from experiments corresponding to the data in Figs. 5(d) and (e) are shown respectively.

In summary, the feasibility of parallel sperm sorting with the annular laser trap has been demonstrated. Under a specific laser power, two groups of sperm could be significantly differentiated ($p \ll 0.05$) based on their VAP or VCL. By

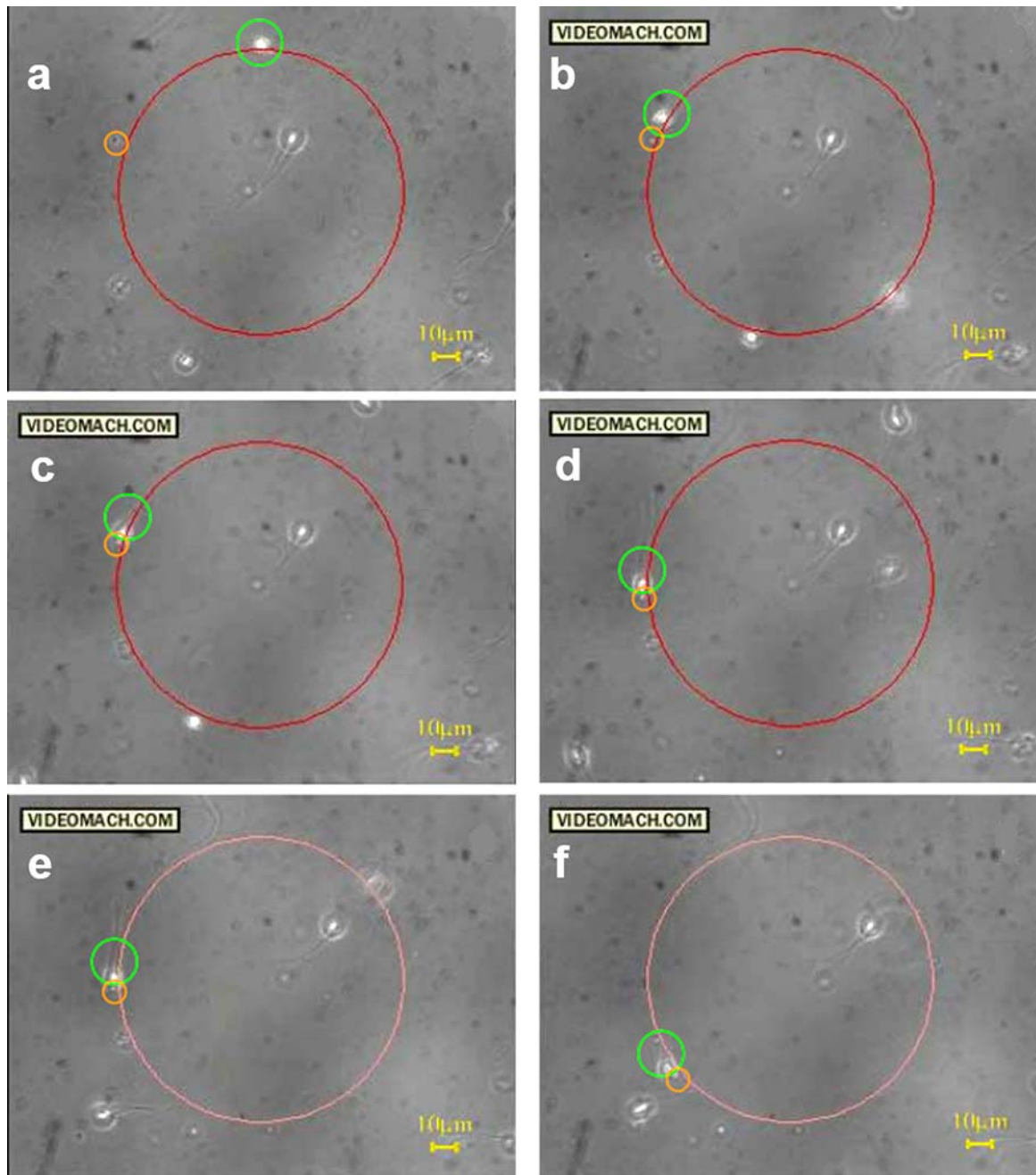


Fig. 6 Sequences of images showing a sperm pushing cell debris while it is swimming along the ring trap. (a) frame #8, under a laser power of 25 mW per sperm, a sperm (medium circle) is swimming along the ring (big circle) counterclockwise, while a cell debris is trapped by the ring (small circle). (b) frame #92, right before the sperm touch the debris. (c, d) frame #115 and #199, the sperm keep swimming along the ring by pushing the debris forward. (e, f) frame #385 and #469, the laser

power is reduced to 20 mW per sperm, the sperm keep swimming along the ring with the load. The time interval between (a) and (b), (c) and (d), (e) and (f) are identical, therefore the change of sperm swimming velocity could be clearly seen by examine the difference of circumferential displacement of the sperm, which is in agreement with Fig. 5(d). The different colors of the big circle correspond to different power level (dark-high power, light-low power)

confining a sperm’s swimming along the ring, the impacts of external transversal force (magnitude—“power binary” and “power gradient”, applying period—“fatigue”) and obstacles (“load” and “block”) on sperm motility were studied. While most sperm experience degradations in VAP and VCL under

a larger laser dose or a longer period of transverse force, the relationship between ALH and transverse force has not been clarified. The observation of “fatigue” after 20 s is in agreement with previous research using a single spot laser trap (Nascimento et al., 2006).

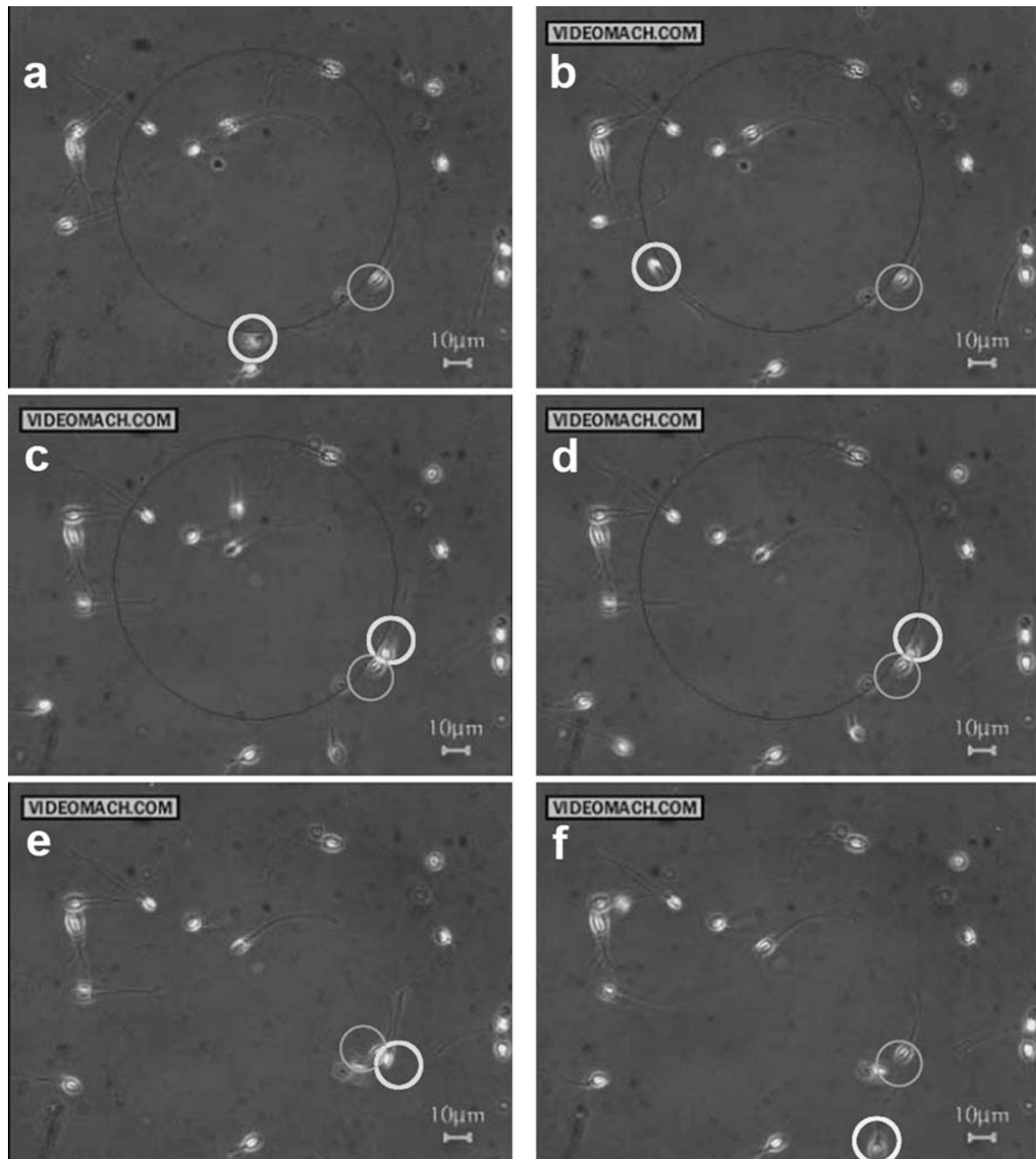


Fig. 7 Sequences of images showing a sperm blocked by a dead sperm while it is swimming along the ring trap. (a), (b) frame #1 and #51, under a laser power of 23 mW per sperm, a sperm (small white circle) is swimming along the ring (big dark circle) clockwise. A dead sperm stuck to the glass is on the ring (small grey circle). (c, d) frame #325 and #375, the sperm encounters the dead sperm and could not keep

moving forward. (e, f) frame #425 and #475, after the laser is turned off, the sperm is able to change its head orientation, bypass the dead sperm and swim away. The time interval between (a) and (b, c) and (d, e) and (f) are identical, therefore the change of sperm swimming velocity could be clearly seen by examine the difference of circumferential displacement of the sperm, which is in agreement with Fig. 5(e)

4 Discussion and conclusions

According to the almost linear relationship between laser trapping power and sperm motility (Tadir et al., 1990; Nascimben et al., 2006) it is possible to adjust the average trapping power per sperm so that different thresholds are used

for multi-level sorting. When the total input power is limited or fixed, a diameter change of the annular trap leads to a variation of the trapping powers per spot. This could be achieved by adding two more axicons between the focusing lens and the tube lens, and changing their axial separation (Shao et al., 2006). As a result, sperm with different motility will escape

the trap at different times. Additionally, since the size of sperm may vary between species, the re-sizing ability of the ring-shaped trap should make it possible to study different species without redesign of the optics. Finally, a resizable ring can be used to study the diffusion length of an attractant and the effect of the curvature of external transverse force on sperm swimming.

In the current study, the sperm in the chamber swim in random directions. This condition could be changed by introducing a chemo-attractant, such as ovary extracts to the center of the ring trap. Chemotaxis is a critical feature of sperm in response to the diffusion gradient of chemicals released by the egg and surrounding cells of the cumulus oophorus. Sperm should start approaching the chemo-attractant from all directions. As a result, the annular trap could be used to sort sperm according to their chemotactic response.

For both motility and chemotaxis sorting, the final goal is to use the classified groups of sperm for later analysis, which is promising with the aid of a microfluidic system.

In conclusion, the annular laser trap provides the possibility of multi-level, high-throughput sperm sorting based on motility and chemotaxis. With only tens of milliwatts devoted to each sperm, this new type of laser trap offers a more gentle approach to sperm analysis and laser-sperm interaction study. The strong optical gradient in the radial direction and the zero gradient force in the circumferential direction make it possible for a sperm to swim along the ring without having to stop. As a result, the effect of optical force, laser radiation and external obstacles on sperm swimming pattern can be investigated in more detail. The unique geometrical feature of the “ring” also provides a way to confine a swimming cell in the field of view for an extended period of time without having to deal with sharp turns or changes in swimming curvature. Earlier research has shown that sperm motility parameters and fertility potential increase with mitochondrial membrane potential (Kasai et al., 2002). With the aid of specific fluorescence probes, such as JC-1 and DiOC₂(3), etc., the membrane potential change of a sperm can be monitored while it is swimming along the ring. These data when combined with measured changes in swimming parameters, can be used to evaluate the motility change of a sperm in response to laser trapping. The applications could

be extended to motility and bio-tropism studies of other self-propelled cells, such as algae and bacteria.

Acknowledgments This work was supported by funds from the Scripps Institute of Oceanography, the US Air Force Office of Scientific Research (AFOSR # F9620-00-1-0371 to MWB), and the Beckman Laser Institute Inc. Foundation. The authors would like to thank IGO Medical Group for providing semen samples from humans.

References

- J.E. Araujo, Y. Tadir, P. Patrizio, T. Ord, S. Silber, M.W. Berns, and R.H. Asch, *Fertil. Steril.* **62**, 585 (1994).
- J. Baumber and S.A. Meyers, *J. Androl.* **27**, 459 (2006).
- Z.N. Dantas, E. Araujo, Jr., Y. Tadir, M.W. Berns, M.J. Schell, and S.C. Stone, *Fertil. Steril.* **63**, 185 (1995).
- S. DiMarzo and J. Rakoff, *Fertil. Steril.* **46**, 470 (1986).
- S. DiMarzo, J. Huang, J. Kennedy, B. Villanueva, S. Hebert, and P. Young, *Am. J. Obstet. Gynecol.* **162**, 1483 (1990).
- M. Eisenbach and I. Tur-Kaspa, *BioEssays* **21**, 203 (1999).
- T. Kasai, K. Ogawa, K. Mizuno, S. Nagai, Y. Uchida, S. Ohta, M. Fujie, K. Suzuki, S. Hirata, and K. Hoshi, *Asian J. Androl.* **4**, 97 (2002).
- K. Konig, L. Svaasand, Y. Liu, G. Sonek, P. Patrizio, Y. Tadir, M.W. Berns, and B.J. Tromberg, *Cell Mol. Biol. (Noisy-le-grand)* **42**, 501 (1996).
- A. Lafong, W.J. Hossack, and J. Arlt, *Opt. Express* **14**, 3065 (2006).
- J.M. Nascimento, E.L. Botvinick, L.Z. Shi, B. Durrant, and M.W. Berns, *J. Biomed. Opt.* **11**, 044001 (2006).
- P. Patrizio, L. Yagang, G.J. Sonek, M.W. Berns, and Y. Tadir, *J. Androl.* **21**, 753 (2000).
- P.J. Rodrigo, V.R. Daria, and J. Gluckstad, *Opt. Lett.* **29**, 2270 (2004).
- P. Serfini and R.P. Marrs, *Fertil. Steril.* **45**, 854 (1986).
- B. Shao, J.M. Nascimento, E.L. Botvinick, M.W. Berns, and S.C. Esener, *Appl. Opt. (Information Photonics)* **45**, 6421 (2006).
- B. Shao, Ph.D. Dissertation (University of California, San Diego, San Diego, 2006).
- Z. Shi, E.L. Botvinick, and M.W. Berns, in *Cell Motility III: The American Society for Cell Biology*, (San Francisco, 2005).
- Y. Tadir, W.H. Wright, O. Vafa, T. Ord, R.H. Asch, and M.W. Berns, *Fertil. Steril.* **52**, 870 (1989).
- Y. Tadir, W.H. Wright, O. Vafa, T. Ord, R.H. Asch, and M.W. Berns, *Fertil. Steril.* **53**, 944 (1990).
- G. Taylor, *Proc. R. Soc. Lond. A* **209**, 447 (1951).
- The Ethics Committee of the American Fertility Society, *Fertil. Steril.* **53**, 1S (1990).
- R.C. Toffle, T.C. Nagel, G.E. Tagatz, S.A. Phanse, T. Okagaki, and C.A. Warrin, *Fertil. Steril.* **43**, 743 (1985).
- M.M. Wang, C.A. Schnabel, M. Chachisvilis, R. Yang, M.J. Paliotti, L.A. Simons, L. McMullin, N. Hagen, K. Lykstad, E. Tu, L.M. Pestana, S. Sur, H. Zhang, W.F. Butler, I. Kariv, and P.J. Marchand, *Appl. Opt.* **42**, 5765 (2003).